

# Direct Force Measurement and Loading on Developing Tissues in Intact Avian Embryos

Chon U Chan<sup>1,3,5</sup>, Fengzhu Xiong<sup>1,2,4,5,\*</sup>, Arthur Michaut<sup>2</sup>, Olivier Pourquie<sup>2,\*</sup>, L. Mahadevan<sup>1,\*</sup>

<sup>1</sup>John A. Paulson School of Engineering and Applied Sciences, Harvard University, Cambridge, MA 02138

<sup>2</sup>Department of Pathology, Brigham Women's Hospital and Department of Genetics, Harvard Medical School, Boston, MA 02115

<sup>3</sup>Institute of Molecular and Cell Biology, A\*STAR, Singapore 138673

<sup>4</sup>Wellcome Trust / CRUK Gurdon Institute, University of Cambridge, Cambridge, United Kingdom, CB2 1QN

<sup>5</sup>These authors contributed equally to this work.

\*[fx220@cam.ac.uk](mailto:fx220@cam.ac.uk); [pourquie@genetics.med.harvard.edu](mailto:pourquie@genetics.med.harvard.edu); [lmahadev@g.harvard.edu](mailto:lmahadev@g.harvard.edu)

## Abstract

**Developmental morphogenesis is driven by tissue stresses acting on tissue rheology. Direct measurements of forces in small tissues (100µm-1mm) *in situ* such as in early embryos require high spatial precision and minimal invasiveness. Here we report tissue force microscopy (TFM) integrating a vertical cantilever probe and live imaging to enable close-loop control of mechanical loading in early chicken embryos. By testing previously qualitatively characterized force-producing tissues in the elongating body axis, we show that TFM quantitatively captures stress dynamics with high sensitivity. TFM also provides the capacity of applying a stable, non-invasive and physiologically relevant load to drive tissue deformation, which alters morphogenetic progression and cell movements. Together, TFM addresses a key technological gap in tissue force measurement and manipulation in small developing embryos, and promises to contribute to the quantitative understanding of complex multi-tissue mechanics during development.**

Using embedded soft alginate gels, we previously detected a pushing force from the axial tissues (neural tube and the notochord) of early chicken embryos (HH8-12,<sup>1</sup>) that drives body elongation and cell movement near the posterior progenitor domain (Figure 1A)<sup>2</sup>. This pushing force was estimated to be quite small as only very soft alginate gels show marked deformation. The gels were not suitable for accurate quantification of the force as they were heterogenous, irregularly deformed and might undergo mechanical property changes in the chemical environment of the developing embryo. Another general issue with large-size (several to dozens of cell diameters) embedded sensors/actuators is that they cause a large deformation at the local embedding site which could alter the cell organization and tissue mechanics of the normal tissue environment.

One way to minimize the tissue impact of force sensors is to use ultra-thin, retrievable probes, which reduces the size and duration of contact required for the measurements. We considered the cantilever deflection approach<sup>3</sup>, which utilizes a beam/needle that is bent when one end is held still and the other end is under a load. The key of accuracy for a cantilever is the precision of the deflection measurement, which comes from the positional difference between the holding end and the loaded end. To match the sensitivity required for the small stresses produced by soft body axis tissues in the early chicken embryo, we used commercially available atomic force microscope (AFM) silicon-nitrate probes as our cantilevers. These probes can have low spring constants to the order of 0.01N/m (10nN/µm to put in the small tissue perspective). In contrast

to the tapping mechanism in AFM surface imaging, we position these thin ( $\sim 1\mu\text{m}$ ) cantilevers vertically to allow direct insertion into the tissue, with or without modifications to the tip. In the case of measuring the axial pushing force, because the tissue cross-section is much larger than that of the cantilever tip, we glued a tailored piece of aluminium foil ( $200\mu\text{m}$  square,  $\sim 15\mu\text{m}$  thick) to the tip<sup>4</sup>, which fully blocks the elongating neural tube and notochord in a HH11 chicken embryo upon insertion. The embryo (prepared using the *ex ovo* EC culture protocol on a piece of windowed filter paper<sup>5</sup>) is mounted on a glass bottom dish and imaged from below (Figures 1A, S1). The glass bottom dish contains a thin layer of culture gel to support the embryo, and the embryo is covered by a thin layer of PBS and mineral oil to prevent drying<sup>4</sup>. The whole stage is set in an environmental enclosure maintaining  $37.5^\circ\text{C}$  with heating fans. Embryos develop normally at a slightly lower rate for at least 6 hours under these conditions as assessed by somite formation and axis elongation ( $\sim 2\text{hrs}$  per somite as opposed to the  $\sim 1.5\text{hrs}$  normal rate,  $\sim 100\mu\text{m/hr}$  elongation speed as opposed to the  $\sim 150\mu\text{m/hr}$  normal rate). Notably, the probe insertion site heals quickly after cantilever retraction and becomes barely distinguishable in a few minutes. The inverted microscope (10x objective) captures images of the tissue section where the probe tip/attached foil is in focus and sends them to the computer for real-time segmentation to measure the tip position.

To enable dynamic positioning of the cantilever, the chip holding the cantilevers is mounted on an electric piezo (Figure S2). To enable precise measurement of the chip/piezo position, they are further flanked with a pair of capacitors (Figures 1B-C). The capacitance difference between the pair is highly sensitive to the distance between the capacitor plates therefore the movement of the piezo. Before loading the embryo, the chip position and the capacitance reading are first calibrated with the microscope to create a lookup function where capacitance difference is interpreted as chip position. This real time position information can feedback to the voltage controller connected to the piezo as a closed loop system (Figures 1B-D, methods). Voltage can thus be adjusted automatically if any drift of the piezo/chip is detected ensuring the stability of chip position. Extended imaging of the chip confirms that the feedback loop maintains stable chip positioning.

By taking the position differences between the foil (measured by the microscope) and the chip (measured by the capacitors) over time, and multiplying the cantilever spring constant ( $0.2\text{N/m}$ ) and dividing by the foil cross-sectional area, we found the axial elongation stress to be  $\sim 100\text{Pa}$  (Figures 1D-F). Cells are observed to accumulate anterior to the foil as the foil moves and eventually stalls (Movie S1). Posterior to the foil the cell density markedly reduces, analogous to the effect of a water dam cutting off flow (Figure 1F). These results are consistent with our previous gel deformation experiments to detect the axis elongation force<sup>2</sup>. We next measured the stress produced by the neighbouring posterior presomitic mesoderm (pPSM). We positioned the probe next to the pPSM after surgically removing a portion of the posterior notochord (Figure 2A). pPSM tissue is known to undergo expansion and will fill into this opening after surgery<sup>2</sup>. A small stress in the range of  $10\text{-}100\text{Pa}$  is detected which gradually dissipates over several hours (Figures 2B-C). This is consistent with our previous observations that the pPSM compresses on axial tissues and that the compression disappears at the differentiating anterior PSM (aPSM) level<sup>2</sup>. Our system thus enables direct quantitative confirmation of the small forces generated by the tissues of the elongating chicken body axis.

To perform controlled mechanical perturbations, we used the feedback loop to move the piezo/chip to maintain a constant deflection by comparing with the tip position obtained with live segmentation of the tip images. This enables a sustained constant force to be applied to the tissue through the cantilever tip. Using this system, we loaded an anterior to posterior steady pulling force (200nN) on the axial tissues which at the same time is also a pushing force on the posterior progenitor domain (Figure 3A). The embryo shows accelerated elongation under this load and surrounding tissues exhibit differently patterned deformations (Movie S2). We labelled cell clusters in the pPSM and followed their movements by cell tracking (Figure 3A). The stress loading causes the cell cluster to move more laterally, following the “U” shaped trajectory from the progenitor domain to the pPSM (Figure 3B), consistent with more invasive approaches such as a magnetic pin that produces excess stresses beyond the physiological range<sup>2</sup>. These data show that in an intact embryo, tissue stresses exerted at one location has wide impacts through inter-tissue connections and alters cell behaviors at a distance, highlighting the importance of integrated multi-tissue models in developmental morphogenesis.

We term the close-loop mechanical system including the vertical cantilever, the piezo, the capacitors, live imaging and incubation described here as Tissue Force Microscopy (TFM, Figure S1). TFM reaches a sensitivity of 1nN (limited by the resolution and accuracy of tip imaging and tracking) and has 3D coverage at ~20µm spatial resolution (typical widths of the probe tip) parallel to the stress and 1-30µm along the direction of the stress (depending on how the tip is modified, such as fluorescence, foil, etc). A stress measurement against a deforming tissue takes 10-30min to reach stalling. The sharp tip creates little tissue damage (such as tearing) even with a strong stress load. These features are advantageous as the tissues are measured more closely to their native state with no large local deformation caused by implants such as gels or droplets. By applying a well-controlled stress close to the endogenous force of the tissue *in vivo*, downstream cellular responses such as gene expression changes can now be studied in more physiologically relevant ranges and at reduced experimental noises that are often difficult to achieve with mechanical perturbations. Combining TFM loading with genetic probes would also allow the molecular force reporters to be calibrated<sup>6</sup>. The requirement of bottom microscopy and therefore a thin flat sample like the early chicken embryo can be overcome with self-detecting probes or alternative deflection detectors such as an interferometer. Future work will aim at improving the automation and throughput of TFM and expanding its applications to rheological measurements and other model systems. TFM shows promise as a broadly useful method adding to the expanding toolbox<sup>7</sup> for understanding the physical mechanisms of morphogenesis and quantitative engineering of development in small tissues.

**Author contributions:** C.U.C. and F.X. conceived the method with inputs from A.M, O.P. and L.M.; C.U.C. designed and constructed the TFM with F.X.; A.M. contributed to hardware components and the oil incubation protocol. C.U.C. and F.X. performed the experiments. F.X. analysed the data and wrote the manuscript.

**Acknowledgements:** We thank S. Gapon, A. Mongera, and C. Guillot for logistical and technical assistance. This work is supported by an A\*STAR International Scholarship to C.U.C., a NIH K99 award (HD092582) and a Wellcome Trust / Royal

Society Fellowship (215439/Z/19/Z) to F.X., and a NIH R01 (HD097068) to O.P. and L.M.

## Materials and Methods

**Eggs and embryo preparation.** Wild type chicken eggs were supplied by Charles River Laboratories. Tg(CAG-GFP)<sup>8</sup> chicken eggs were provided by Clemson university (originally by University of Edinburgh). Eggs were kept in monitored 15°C fridge for storage and 37.5°C ~60% humidity egg incubators for incubation. HH stage 10-12 embryos were used. The early-stage embryos are used under a tissue protocol and do not require an animal protocol per institution guidelines. To obtain the embryos for TFM measurements, eggs were incubated for ~40 hours before opening for the EC culture<sup>5</sup>. The EC culture uses 2cm x 2cm pieces of filter paper (Whatman) with two adjacent 0.5cm holes in the center. Eggs were opened into a petri dish and the thick albumen on the top that covers the embryo and the vitelline membrane is swept aside gently with small filter paper pieces using a tweezer. The holed filter paper is then lowered to attach to the vitelline membrane where embryos are visible through the hole (body axis aligned to the long axis of the hole). The vitelline membrane is then cut around the filter paper to release the embryo. The filter culture embryo is then rinsed in PBS to remove excess yolk. The cleaned embryo is then placed on a 3.5cm petri dish containing 2ml of culture gel made with the following formula (per 100ml of culture gel): Part A: 50ml Albumin (beaten for 15min) then supplement with 0.8ml 20% D-Glucose (Sigma); Part B: 0.3g BactoAgar (Sigma) solved in 50ml water in a microwave then supplement with 1.23ml 5M NaCl. Warm part A and cool part B to 55°C in a water bath. Mix thoroughly and add to petri dishes (2ml each) before gelation. The embryo cultures are then stored in a slide box with wet paper towels in the incubator. In experiments where some tissue areas and cells are labelled by Dil, the Dil was injected with a sharp-tipped glass needle by mouth pipetting from the ventral side of the embryo. The stock solution of 2.5mg/ml Dil in ethanol was diluted in PBS to 0.5mg/ml before injection. At the sample loading step of the TFM procedure (see below), two embryos are taken and transferred to a pre-warmed glass bottom imaging dish (MatTek) covered with 200µl of culture gel. A second piece of filter paper is then added to prevent the embryo from detaching and floating once it's submerged. Pre-warmed PBS was then added to cover the embryos, followed by 1-2 drops of mineral oil just enough to spread and cover the surface. One embryo is subjected to TFM measurements/loading while the other serves as a control inside the incubation chamber on the scope.

**Design and Operation of the TFM.** A working TFM can be assembled with the list of required equipment and components below. Design considerations are described and the components used in this study are listed, but it is not necessary to acquire the same components. The construction of the probe holder and incubation chamber would depend on the configuration of the base microscope that's used. Similarly, existing microscope software can be incorporated into the operation procedure. Users with electrical engineering and programming experiences are required for the assembly and maintenance of the system.

### 1. Required equipment and components

**1.1 Microscope.** To construct a TFM system, an inverted microscope with XY stage control and Z focus control is required. We used the Zeiss Axio Observer base (top

modules including the TL illumination and condenser are removed). A low magnification objective 2.5-5x is required for sample positioning and a 10x objective is required for image data streaming.

1.2 Camera. Due to the lack of TL illumination and the size and close proximity of the probe holder to the sample, side LEDs were included to compensate for the lack of light on the sample. A sensitive, fast camera is required to provide high resolution streaming of the probe tip in the tissue, which is essential for real-time feedback control of the force. The system's temporal and spatial resolution limit is set by the camera and imaging protocol (described in more detail in section 4). We used a Ximea USB camera (MQ042MG-CM).

1.3 Custom probe holder and capacitors. A stable, controllable probe needs to be installed on a reliable micromanipulator/stage as a holder with minimal drift over time. We used a World Precision Instruments WPI M3301R Manual Micromanipulator and a Newport Corp. 9062-XYZ-M stage. The stage was fixed to optical rails and beams (Thorlabs) onto the microscope base, forming an overhang on top of the sample stage. We 3D-printed 2-part plastic holders where the sample side has a slot for the chip of AFM probes and the piezo side has a slot for the insertion of the mobile end of the piezo ([Figure S2](#)), and two slots on either side for the mobile copper capacitor plates. The 2 parts are tightened with screws to allow piezo and probe exchanges. The static end of the piezo is inserted in another printed holder which connects to a cage that holds the fixed capacitor plates. The capacitors flank the piezo whose positioning affects the capacitance difference ([Figures 1B-C](#)), allowing a calibration of capacitance to holder position at the beginning of an experiment (described in more detail in section 4).

1.4 Voltage controller and piezo. A programmable voltage controller is required to drive the piezo. We used a custom built one integrating a low and high power source but commercial ones such as Thorlabs (MDT694B) would also work. The controller needs to be able to adjust voltage output quickly and accurately during live measurements to enable the feedback control. The piezos we used are the ceramic piezoelectric benders from Thorlabs (PB4NB2W). Note that components in 1.3 should be designed in accordance with the type of the piezo and working range required.

1.5 AFM probes. We used smooth (no tip modifications) silicon nitrate AFM probes from Bruker (MLCT-O10) and NanoAndMore (AIO-AL-TL) with spring constants ranging from 0.01-0.2N/m. Comparable probes will be feasible to use. It is advantageous to use probes with a larger length as they can reach deeper points of the embryo.

1.6 Environmental chamber. The embryo requires proper temperature and humidity to develop normally. Common lab and microscope facility environments have a low humidity and room temperature around 25°C. We used a layer of mineral oil to reduce evaporation but this is not the optimal method as long-term survival of the embryo is affected under this condition. Environment chambers where humidity can be maintained at a high level while the electronics still function would be desirable. Alternatively, oxygenating the culture media that submerges the embryo may also be effective. We used a custom laser-cut cardboard box to enclose the holder and the sample stage and heating fans integrated with temperature sensors to maintain

37.5°C. Commercially available environmental chambers would also work but customization (e.g. additional holes) are needed to allow the installation of the probe holder and the in/out wires.

## 2. Optional components

2.1 Microcontroller. Because multiple data streams (images, capacitance, voltage, temperature, etc) flow through the system, it is advantageous to organize them under an integrated controller to align data onto the same time axis. For force measurement and loading small time differences in data streams do not cause a major issue because the probe and sample move slowly and errors average out through the feedback over time. However, for other measurements potentially capable by TFM, such as oscillatory rheology, time axis alignment is critical. In these situations, a master clock is used to trigger the camera and capacitance readings for synchronization. We used a Teensy microcontroller to link different parts of the system and interface with Matlab (Mathworks) on the computer.

2.2 Illumination modules. Having good contrast on the probe tip and embryo tissues is important for the precision of tip positioning and position measurement via image segmentation. The overhanging holder including the capacitors and the piezo form an occlusion for overhead TL illumination. Small LEDs can be installed on the holder to directly illuminate the sample. We used side LEDs which are fixed on the sample stage. The LEDs can be triggered by the camera or the microscope. We also used the fluorescence module of the Zeiss scope to provide RL illumination on the GFP transgenic embryos, and the probe tip which can be coloured by Quantum dots glued on via epoxy, or simply taking advantage of the autofluorescence of epoxy.

3. Software. To measure and control forces, the locations of the chip and the tip are streamed in real time, and the chip location can be altered with piezo movement. Therefore, the main functionalities to achieve with the software are to send and receive the chip/piezo position (i.e. voltage), to program imaging, receive images and obtain tip position. We used Matlab (MathWorks) to create the user interface that plot the serial data via a USB link to the microcontroller, and to run the image segmentation. For the objective and shutter control we used Micromanager<sup>9</sup>. A Teensy program that integrates the data streams is uploaded to the microcontroller prior to the start of experiments.

## 4. Operation

4.1 Testing and calibration. An assembled TFM system needs to be tested and calibrated prior to loading actual samples. This step ensures the system functions properly and produces necessary parameters and data for the sample measurements. Firstly, holder stability must be tested for the desired duration of the experiment. Without samples, use the microscope to take a timelapse of the overhang holder without (a) and with the voltage controller on (b), and with the capacitor-voltage controller feedback loop on where a set capacitance is sent by the software (c). For a stable system, all timelapse results should show minimal movement of the probe, but the system is usable if (a) is stable and (c) achieves correction for drifts in (b). (a) tests the stability of the scaffold such as the rails, columns and the micromanipulator. (b) tests the stability of the piezo and voltage controller output. (c) tests the capacitor positioning system and the feedback.

Secondly, the correlation between capacitance differences and the position of the holder needs to be established by driving the piezo across its dynamics range while capturing holder movement with timelapse imaging. This data serves as a lookup table that links capacitance reading to holder position, which will be used in sample measurements where the holder position can no longer be measured by imaging because of sample obstruction.

4.2 Sample loading and probe insertion. Because the sample will result in light obstruction and scattering, the microscope view of the probe holder and tip will be blurry, making the probe insertion process difficult to see from the camera. Therefore, the XY position of the probe should be marked on the field of view prior to sample loading. The probe holder is then raised in Z (without touching its XY control) only to make room for the sample. After the sample dish (refer to “embryo preparation” for the protocol of readying a chicken embryo for TFM) is in place, the desired tissue location can be aligned to the mark using the sample stage so that the probe tip will enter the right location once it’s lowered again. Once the probe enters the liquid layers, care must be taken to slowly lower the probe further to the desired tissue depth without overshooting which could cause tip breakage and/or tissue damage. The entrance of the probe/foil into the tissue is usually smooth because of their sharpness. Light conditions may make it difficult to see the location of the probe tip. It’s advisable to adjust the objective focus around the sample plane to find the probe tip. Once the probe is in the proper tissue location and in focus, camera and lighting settings can be further adjusted to ensure good-contrast images at a fast rate (low exposure time).

4.3 Force measurement and loading. To measure tissue forces/stresses, the probe should be inserted to block the direction of tissue movement. If the desired measurement cross-section of the tissue is larger than the probe, a piece of aluminium foil can be attached to the probe tip via epoxy. We cut the foil pieces using a micromanipulator with a blade under a dissecting microscope to obtain rectangular pieces of 100-200 $\mu$ m. To measure the stalling stress, once the tip/foil is in position, the capacitance should be fixed through the feedback loop to maintain the position of the holder. Timelapse imaging of the tissue area and the tip/foil displacement then indicates the force. The displacement will increase quickly then slowly and finally stall as morphogenesis is stalled by the probe. To load the tissue with a specific force, the force value will be evaluated against the current probe location and capacitance reading, and an adjustment of capacitance target (therefore holder position) will be sent to the voltage controller. With continued imaging and segmentation on the fly, the feedback loop maintains a dynamically stable difference between the holder and the probe tip (therefore cantilever deflection and force). After completion of measurements, the probe should be washed in deionized water by dipping to prevent damage from culture gel, albumen and salt crystals after drying.

**Data analysis.** Movies were analyzed in Fiji (ImageJ). Probe/foil displacement was measured by object tracking in the intensity-time plot. The fluorescence intensities (as a proxy to cell density) were measured by drawing a ROI before and after the foil. Dil labelled cells were tracked with the Manual Tracking plugin. Tracking results and measurements were processed in Matlab (Mathworks) with custom scripts and plotted with Excel (Microsoft).

## References

1. Hamburger, V. & Hamilton, H. L. A series of normal stages in the development of the chick embryo. *J. Morphol.* **88**, 49–92 (1951).
2. Xiong, F., Ma, W., Bénazéraf, B., Mahadevan, L. & Pourquié, O. Mechanical Coupling Coordinates the Co-elongation of Axial and Paraxial Tissues in Avian Embryos. *Dev. Cell* **55**, 354-366.e5 (2020).
3. Hara, Y. *et al.* Directional migration of leading-edge mesoderm generates physical forces: Implication in *Xenopus* notochord formation during gastrulation. *Dev. Biol.* **382**, 482–495 (2013).
4. Michaut, A. Biomechanics of anteroposterior axis elongation in the chicken embryo. (2018). <https://www.theses.fr/2018STRAJ075>
5. Chapman, S. C., Collignon, J. J., Schoenwolf, G. C. & Lumsden, A. Improved method for chick whole-embryo culture using a filter paper carrier. *Dev. Dyn.* **220**, 284–289 (2001).
6. Kim, T. J. *et al.* Dynamic Visualization of  $\alpha$ -Catenin Reveals Rapid, Reversible Conformation Switching between Tension States. *Curr. Biol.* **25**, 218–224 (2015).
7. Campàs, O. A toolbox to explore the mechanics of living embryonic tissues. *Seminars in Cell and Developmental Biology* vol. 55 119–130 (2016).
8. McGrew, M. J. *et al.* Localised axial progenitor cell populations in the avian tail bud are not committed to a posterior Hox identity. *Development* **135**, 2289–2299 (2008).
9. Edelstein, A. D. *et al.* Advanced methods of microscope control using  $\mu$ Manager software. *J. Biol. Methods* **1**, e10 (2014).

## Figures

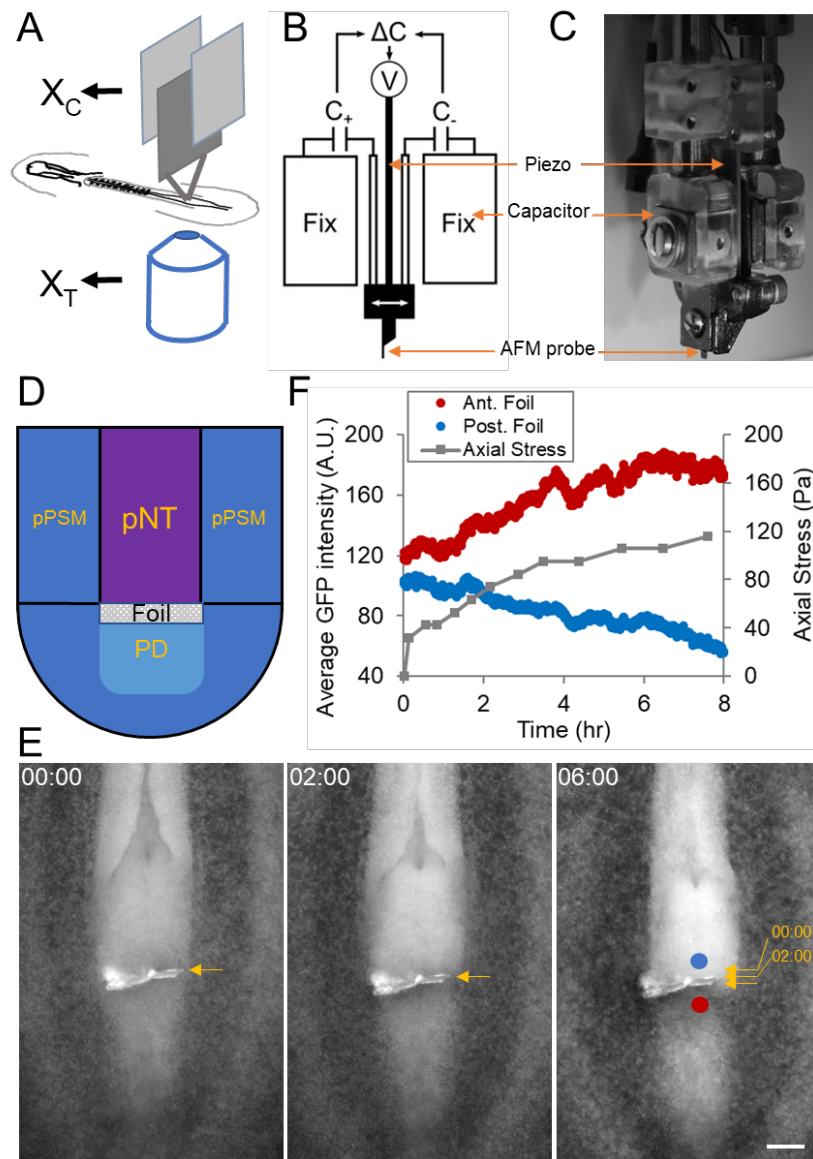


**Figure 1. Tissue force microscope (TFM) to measure the axial elongation force**

(A) Concept of TFM. The design takes advantage of the flatness of the early avian embryo.  $X_C$  is the holder “chip” position measured by the capacitors,  $X_T$  is the probe “tip” position measured by the microscope. Their difference measures the deflection of the cantilever beam.

(B-C) Probe holder and capacitors. Two capacitor plates and the piezo are integrated for position control and measurement against two fixed plates. C, capacitance; V, voltage; (C) is a side photo of the assembled probe holder.

(D) Diagram of the axial elongation measurement. This is a dorsal view of the tail end of the embryo as seen in (E), the probe enters from the ventral side. pPSM, posterior presomitic mesoderm; pNT, posterior neural tube; PD, progenitor domain. Cells from the PD enter the U-shaped PSM under the pushing forces from the pNT and notochord<sup>2</sup>.

(E) Foil movement under the elongation force. Arrows indicate the small displacements of the foil (overlaid on the third image). Blue and Red dots mark the

ROIs for fluorescence intensity measurements. This is a GFP embryo. Neural tube folds can be seen to be closing and narrowing. Representative of 5 similar experiments.

(F) Axial elongation stress and cell density approximated by fluorescence intensity. The stress is calculated by the displacement, the cantilever spring constant (0.2N/m) and the cross-sectional area of the foil. Scale bar: 100 $\mu$ m.

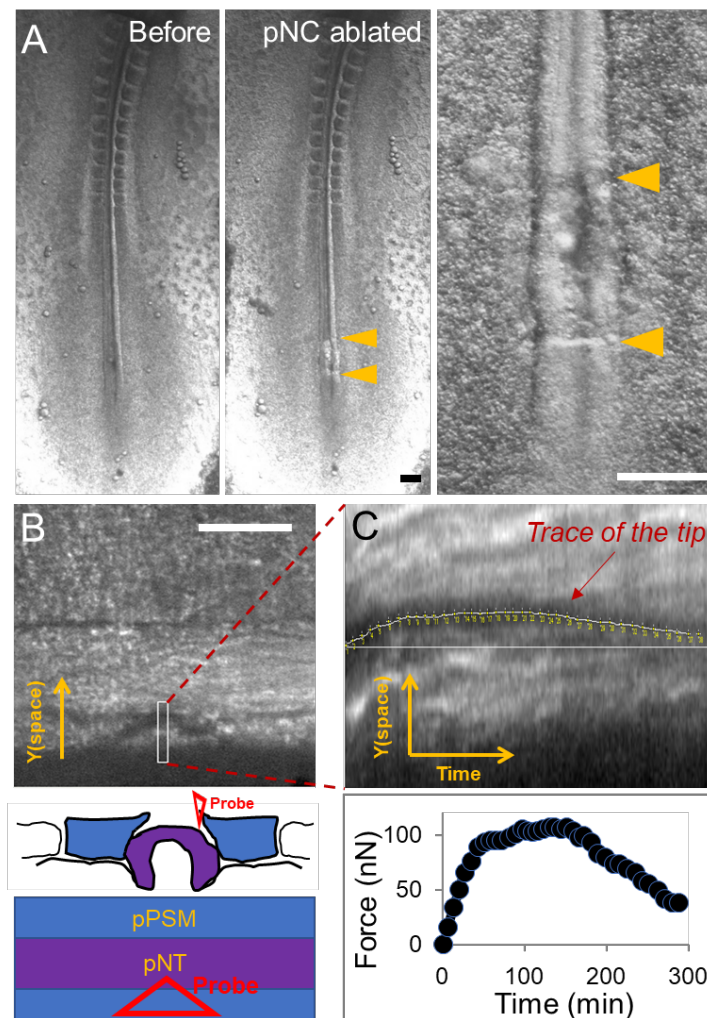


**Figure 2. Measurement of the posterior presomitic mesoderm compression**

(A) Ventral view of a HH11 embryo undergoing posterior notochord (pNC) ablation to reveal the medial surface of the pPSM. Arrowheads mark the anterior and posterior borders of the surgical window. Neural tube which is further dorsal remains intact and is in the view. Representative of 3 similar experiments. Scale bars: 200 $\mu$ m.

(B) Dorsal side view of the region in A now under the TFM. As indicated in the diagram, a soft triangular probe (0.01N/m) is now inserted medially by the pPSM boundary, the shadow of the triangle tip is visible. The pPSM tissue is known to expand into this area after pNC is ablated. Scale bar: 100 $\mu$ m.

(C) Trace of the probe tip shows its deflection over time and translates to the lateral to medial force generated by the pPSM. The force quickly stalls around 100nN and dissipates after a few hours. The estimated contact surface size with the probe is on the order of 10<sup>3</sup>-10<sup>4</sup> $\mu$ m<sup>2</sup>, predicting a pPSM stress in the range of 10-100Pa.

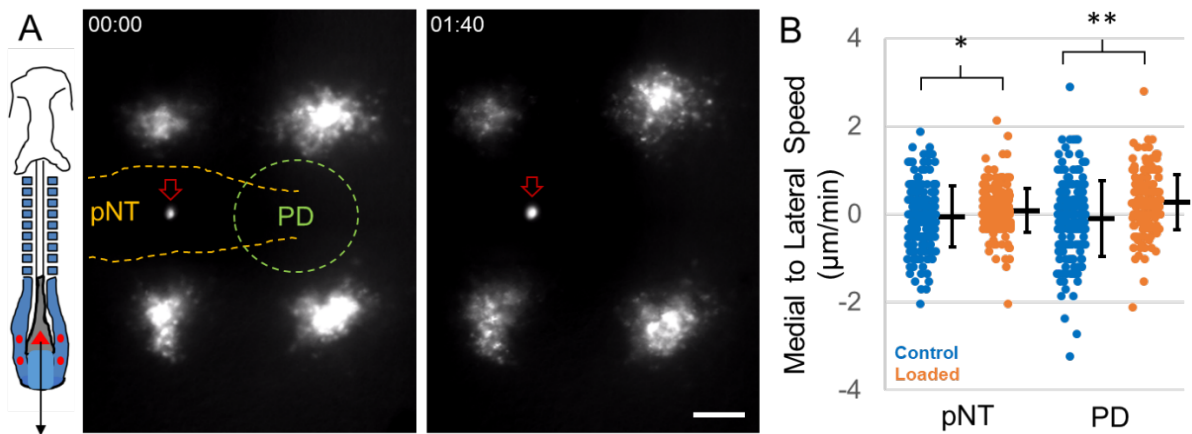


### Figure 3. Cell dynamics following mechanical load

(A) Schematic and images from a loaded and Dil labelled embryo. The red triangle on the image indicates the probe tip, which is also fluorescent in the red channel similarly as Dil (red empty arrow in the images). The black arrow indicates the direction of the force. Red dots mark the Dil injection sites in the pPSM corresponding to the clusters of cells on the image. pNT, posterior neural tube; PD, progenitor domain. 2 clusters are on the same anterior-posterior level as the pNT and 2 as the PD. Some of the Dil labelled cells in these movies can be tracked to analyse cell movements. Representative of 4 similar experiments.

(B) Medial to lateral speeds of cells measured from tracks on the pNT and PD levels, respectively. Each speed measurement is taken by the cell's displacement over a 5 minute interval. Loading causes cells to move more laterally on average. \*, \*\*,  $p < 0.05$ , t-tests.

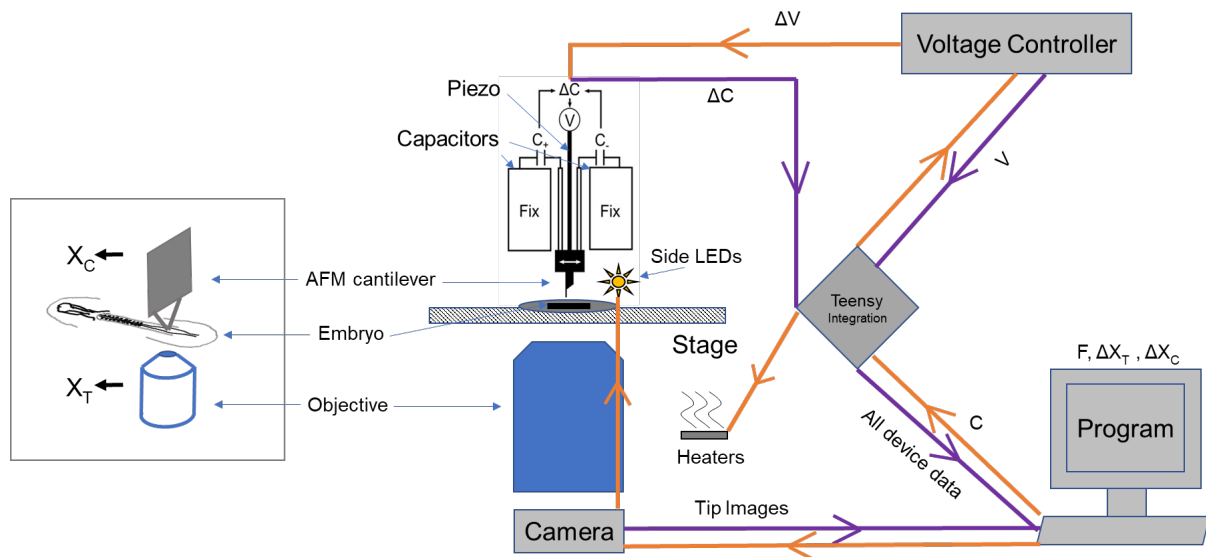


### Figure S1. Diagram of the TFM system

The left image is the conceptual design related to the actual system on the right. Purple arrows indicate data flow from and orange arrows indicate command signals.

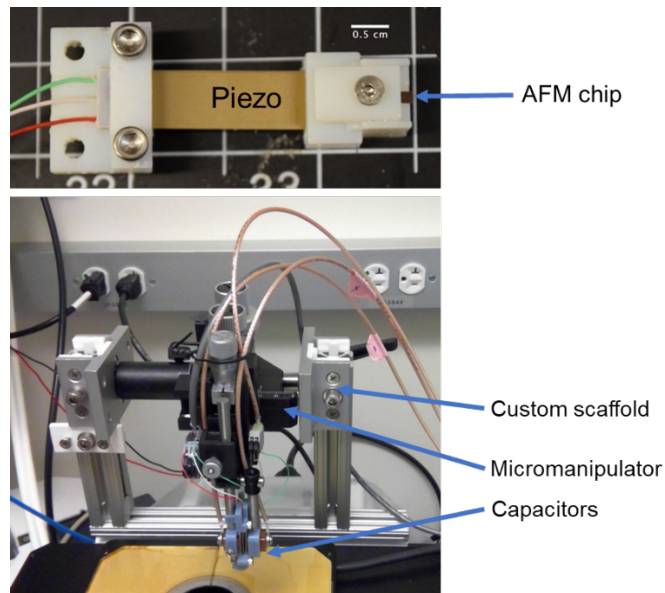


**Figure S2. Custom printed/built parts of the TFM system**

Top image shows the 3D-printed plastic piezo holders. Bottom image shows the overhang scaffold. These designs are flexible with the actual scope and piezo used.

**Movie S1. Measuring axis elongation stress with TFM**

Time stamps are hh:mm. This is a dorsal view of the tail end of a GFP embryo, anterior to the left. Refer to text for further details.

**Movie S2. Force loading on a live embryo**

Time stamps are hh:mm. Two GFP embryos, a control (left) and a loaded one (right) are shown, anterior to the top. Probe tip (modified with epoxy) is visible as a bright sphere with a dark bar in the center in the loaded embryo. The loaded embryo elongates at a faster rate. Refer to text for further details.